Supporting Information

Single-Molecule Observation of Selenoenzyme Intermediates in a Semisynthetic Seleno-α-Hemolysin Nanoreactor

Xiaojia Jiang,[1] Tiezheng Pan, [1] Chao Lang, [1] Chao Zeng, [1] Jinxing Hou, [1] Jiayun Xu,[2] Quan Luo, *[1, 3, 4] Chunxi Hou*[1] and Junqiu Liu* [1, 2]

1. State Key Laboratory of Supramolecular Structure and Materials, College of Chemistry, Jilin University, Changchun 130012, China

2. College of Material Chemistry and Chemical Engineering, Hangzhou Normal University, Hangzhou 311121, China

3. Key Laboratory for Molecular Enzymology and Engineering of Ministry of Education, School of Life Sciences, Jilin University, Changchun 130012, China.

4. Key Laboratory of Emergency and Trauma, Ministry of Education, College of Emergency and Trauma, Hainan Medical University, Haikou 571199, China

Corresponding authors:

Professor Chunxi Hou: chunxihou@jlu.edu.cn.

Professor Quan Luo: luoquan@jlu.edu.cn.

Professor Junqiu Liu: junqiuliu@jlu.edu.cn.

Table of Contents

1. Materials

Tryptone, yeast extract, LB agar, 4-(2-hydroxyethyl)-1-piperazineethanesulfonic acid (HEPES), Decane, TrixonX-100, ampicillin, kanamycin, nicotinamide adenine dinucleotide phosphate (NADPH) and glutathione (GSH) were purchased from Sangon Biotech Co., Ltd.; 1,2-diphytanoyl-sn-glycero-3-phosphocholine (DiPhPC) was purchased from Avanti Polar Lipids; dNTPs and pfu DNA polymerase were purchased from Takara Co., Ltd.; DpnI was purchased from Thermo Scientific Co., Ltd.; E. coli strain BL21 (DE3) and E. coli strain DH5α were purchased from Tiangen Biotech; Isopropyl β-D-1-thiogalactopyranoside (IPTG) and protein Marker(14.4-94.0kDa) were purchased from Solarbio; Ethylenediaminetetraacetic acid (EDTA) and potassium chloride were purchased from Aladdin (China); PCR primers were synthesized from Sangon Biotech Co., Ltd.; various amino acids, rifampin, biotin and chloramphenicol were purchased from Sangon Biotech Co., Ltd. other inorganic salts and hydrogen peroxide (H_2O_2) were purchased from Beijing Chemical Works; Glutathione reductase (GR) was purchased from Sigma-Aldrich. Rabbit red blood cells were purchased from Shanghai Yuduo Biotechnology Co., Ltd. BCA Protein Assay Kit was purchased from Meilunbio. Nicotinic acid was purchased from Beijing ding changsheng biotechnology co., LTD.

2. The construction of seleno-αHL nanopore

The 3D crystal structure of Wild-type αHL was derived from RCSB Protein Data Bank (PDB ID: 7AHL). The procedure of constructing for seleno-αHL was shown in Figure S1.

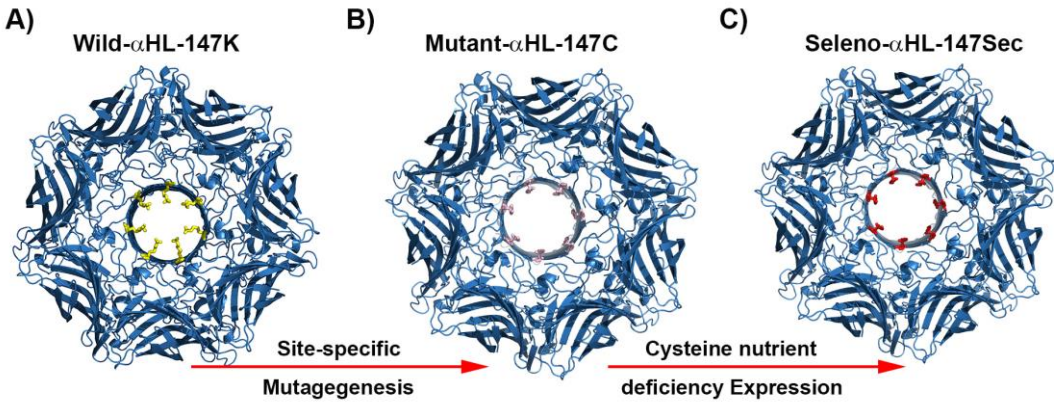

Figure S1. The procedure of constructing for seleno-αHL. A), B) and C) Represented the structure of wild-αHL, mutant-αHL-147C and seleno-αHL-147Sec, respectively, which was analyzed by Pymol software.

3. The theoretical simulation for construction of seleno-αHL nanoreactor

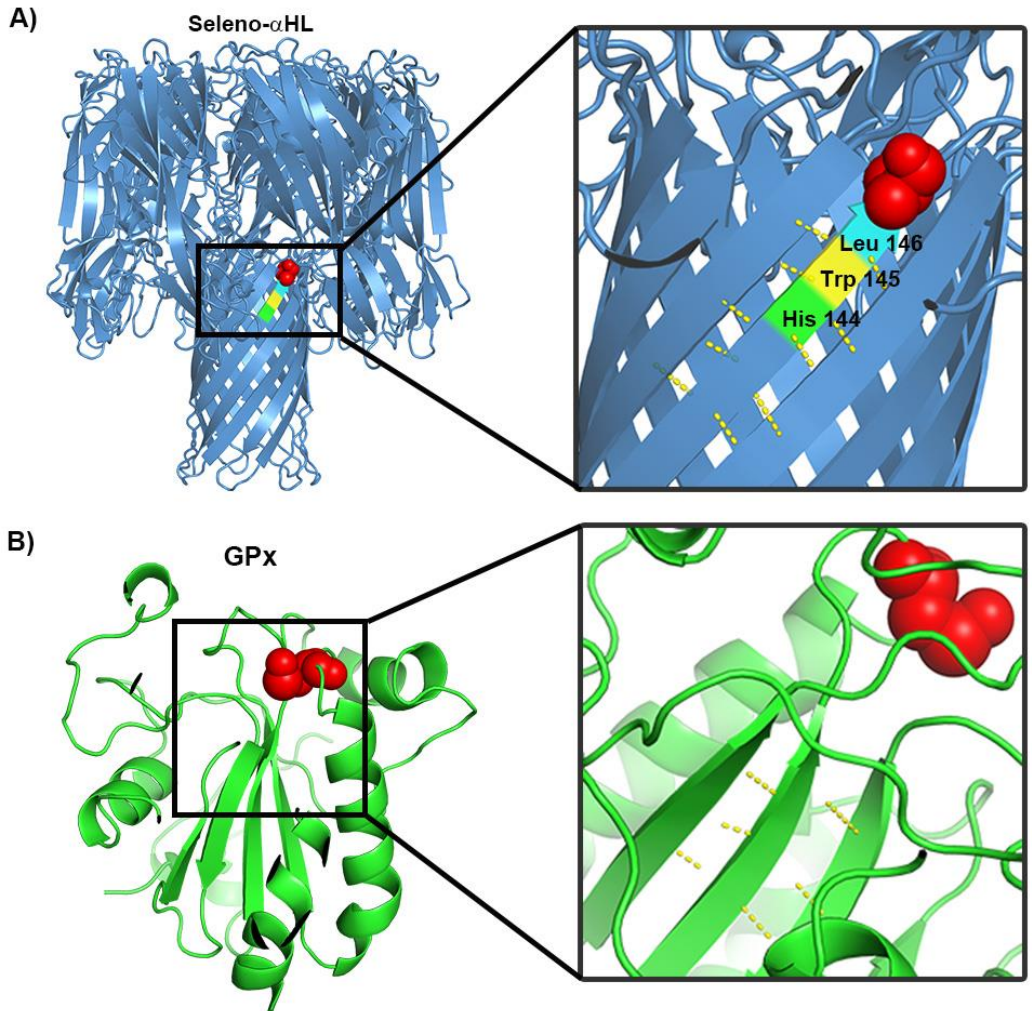

Figure S2. A) The structure of seleno-αHL nanopore and the adjacent amino acids of Sec. B) The structure of natural GPx. Red sphere represented the Sec. The hydrogen bonding of β-strands was marked by the yellow.

4. The theoretical simulation for GSH bound within the lumen of seleno-αHL nanopore

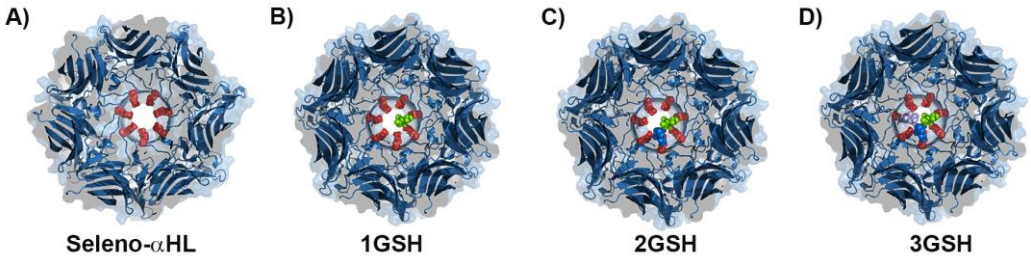

Figure S3. A) Represented the structure of seleno-αHL when different numbers of GSH bound within the lumen of seleno-αHL nanopore. B), C) and D) Represented the different numbers of GSH bound within the lumen of seleno-αHL and the green, blue and purple sphere represent the different GSH respectively.

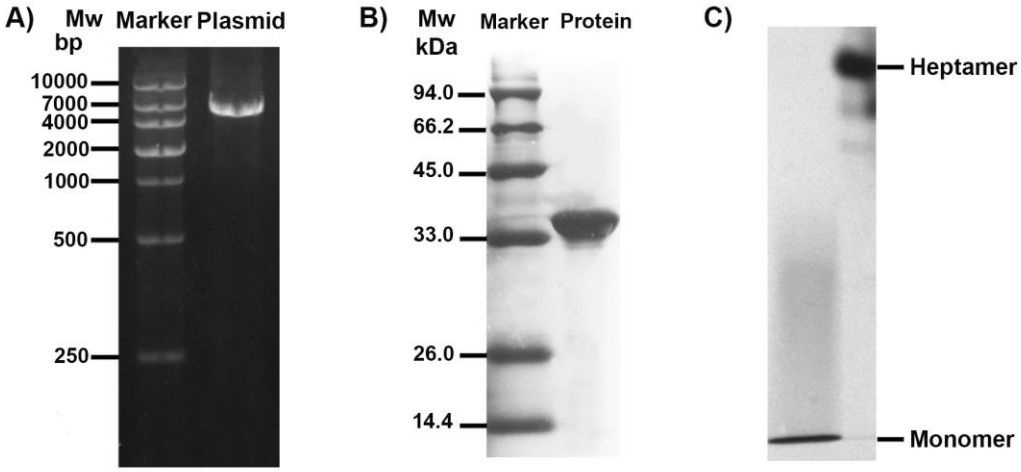

Figure S4. A) The agarose gel electrophoresis of PCR product of mutant αHL (K147C). Left Lane: DNA marker; Right Lane: the plasmid of mutant αHL (K147C). B) The SDS-PAGE analysis of seleno-αHL protein, the left lane indicated the protein marker and the right lane indicated the purified seleno-αHL protein. C) The Native-PAGE analysis of seleno-αHL protein.

5. MALDI-TOF-MS of mutant αHL-147C and seleno-αHL protein

The appropriate difference in molecular weight between wild-type αHL and seleno-αHL protein indicated that we have obtained seleno-αHL protein successfully. Importantly, because that seleno-αHL contains the element of selenium, which could be easily oxidized at atmosphere, the difference in weight between mutant αHL-147C and seleno-αHL protein is referred to the difference between Cys and SeOOH (Figure S5A, S5B).

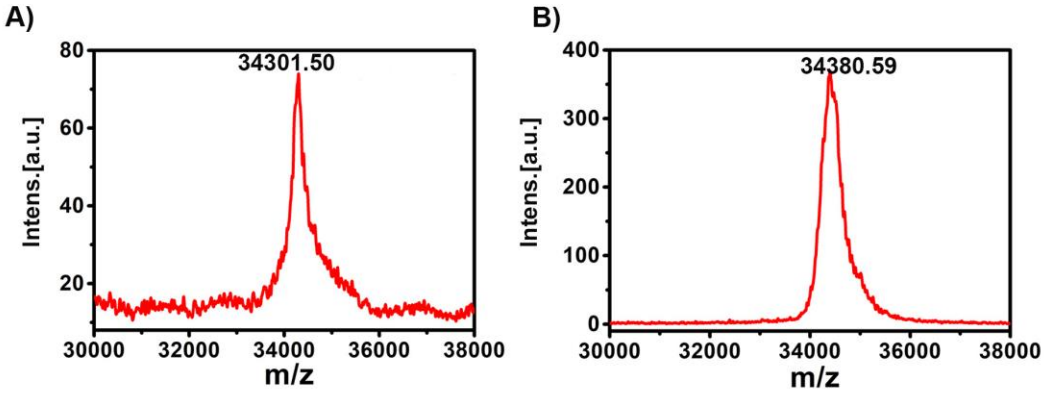

Figure S5. A) The MALDI-TOF-MS spectra of the mutant αHL-147C protein. B). The MALDI-TOF-MS spectra of seleno-αHL protein.

6. Circular Dichroism spectroscopy of the wild-type αHL and seleno-αHL protein

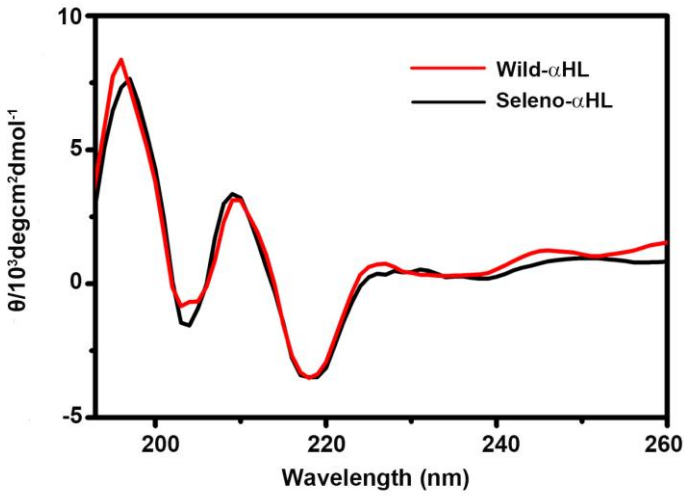

Figure S6. Far-UV circular dichroism spectra. The red line represented wild-type αHL protein and the black line represented the seleno αHL protein.

7. The hemolytic activity of seleno-αHL nanopore

The hemolytic experiments were carried to testify whether the seleno-αHL nanopore maintained the biological activity by adding the final concentration of 0.1 μM seleno-αHL protein into the solution of 0.4% rabbit red blood cells. When the final concentration of 0.1 μM seleno-αHL protein was added into the solution of 0.4% rabbit red blood cells, we found that the red blood cell solution gradually became transparent with the time increased from 0 min to 7 min, which meant that our engineered seleno-αHL nanopore maintained its biological activity. More, the HC_{50} of seleno-αHL nanopore was estimated to be 4 nM (Figure S7), further demonstrated that seleno-αHL nanopore still showed high hemolytic activity as the wild-type αHL nanopore.

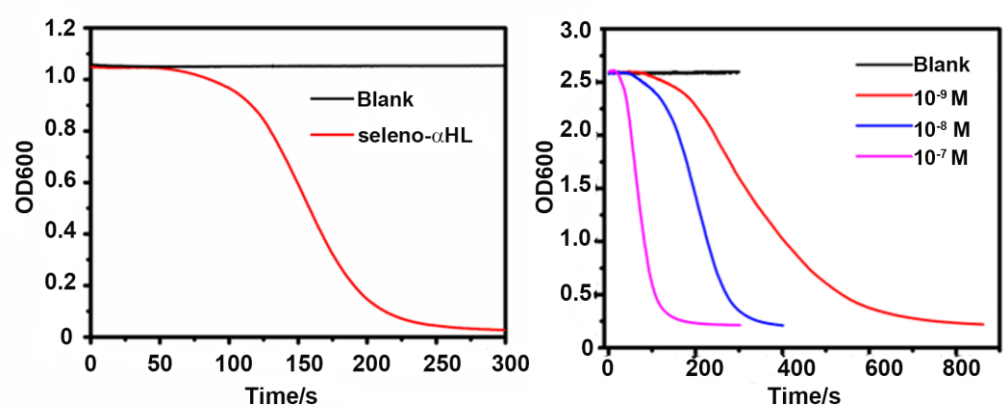

Figure S7. The hemolytic activity of semisynthetic seleno-αHL nanoreactor. Hemolytic experiments were carried out with the different concentrations of seleno-αHL protein added into 0.4% rabbit red blood cells.

8. The GPx activity of semisynthetic seleno-αHL nanoreactor

The GPx-like activity catalyzing the reduction of hydroperoxide (ROOH) by thiols was assessed by using an indirect enzymatic assay (Figure S8).

$$2GSH+ROOH \xrightarrow{\text{GPx mimics}} ROH+GSSG+H_2O$$

$$GSSG+NADPH+H^+ \xrightarrow{\text{GSH Reductase}} 2GSH+NADP^+$$

Figure S8. The catalytic equations of GPx.

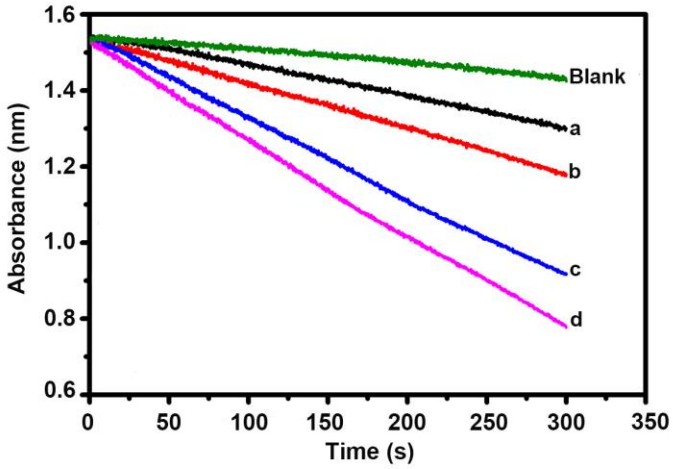

Figure S9. The catalytic curve of semisynthetic seleno-αHL nanoreactor under different concentrations. The concentration ranging from a to d increased.

9. The kinetic parameters and Double-Reciprocal Plots of semisynthetic seleno-αHL nanoreactor

A series of kinetic assays was carried out by varying the concentration of the substrate while keeping the other substrate at a certain level and the apparent kinetic parameters were derived directly from fitting the collected experimental data to the Michaelis−Menten equation (Figure S10).

$$V = \frac{V_{max}\,[S]}{K_m + [S]} \qquad eq.1$$

$$\frac{1}{V} = \frac{K_m}{V_{max}} \times \frac{1}{[S]} + \frac{1}{V_{max}} \qquad eq.2$$

Figure S10. The Michaelis−Menten equation. V_{max} = maximum reaction rate; [S] = substrate concentration: K_m = Michaelis constant: V = reaction rate.

10. The kinetic parameters and Double-Reciprocal Plots of semisynthetic seleno-αHL nanoreactor

The concentrations of GSH in the experiment were 0.25, 0.5, 0.8, 1, and 2 mM, while the concentrations of H_2O_2 were 0.25, 0.5, 0.8, 1 and 2 mM. The apparent kinetic parameters for GSH were deduced, as shown in Table S1 and Table S2 from fitting the experimental data directly to the Michaelis-Menten equation (eq. 1) (Figure S10). Double-reciprocal plots of the initial rate versus substrate concentration displayed a family of the characteristic parallel lines for both substrates (eq.

2). V_{max} = maximum reaction rate; [S] = substrate concentration; K_m = Michaelis constant; V = reaction rate.

Table S1: Kinetic parameters of semisynthetic seleno-αHL nanoreactor

[GSH] (mM)	k_{cat} (min^{-1})	K_{mH2O2} (x 10^{-3})	k_{cat}/ K_{mH2O2} ($M^{-1}min^{-1}$)
0.25	69.99	0.25	2.773 x 10^5
0.5	136.35	0.50	2.748x 10^5
0.8	218.66	0.78	2.786 x 10^5
1	278.77	1.00	2.788 x 10^5

Table S2: Kinetic parameters of semisynthetic seleno-αHL nanoreactor

$[H_2O_2]$ (mM)	k_{cat} (min^{-1})	K_{mGSH} (x 10^{-3})	k_{cat}/ K_{mGSH} ($M^{-1}min^{-1}$)
0.25	69.95	0.25	2.775 x 10^5
0.5	134.40	0.48	2.803 x 10^5
0.8	206.72	0.73	2.849 x 10^5
1	252.07	0.88	2.873 x 10^5

11. Single channel electric recordings of wild-type αHL and seleno-αHL nanopore

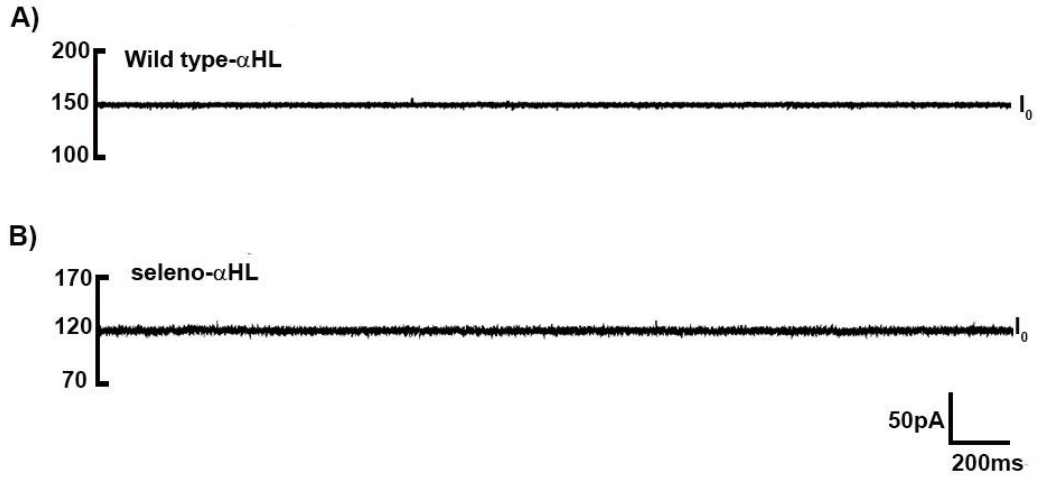

Figure S11. The single channel electric recordings based on wild-type αHL and seleno-αHL. A) The open current of wild-type αHL. B) The open current of seleno-αHL. All nanopore experiments were carried out at +100 mV voltage.

Figure S12. The single channel electric recordings based on wild-type αHL nanopore in the presence of GSH. All nanopore experiments were carried out at +100 mV voltage.

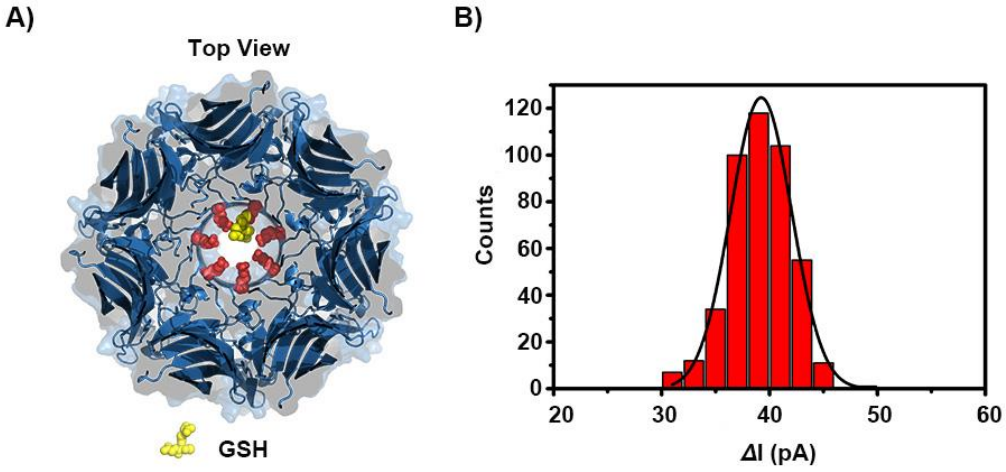

Figure S13. A) Top view when GSH bound within seleno-αHL nanoreactor. B) Event histogram of current blockages of one molecule GSH bound with seleno-αHL nanoreactor. All nanopore experiments were carried out at +100 mV voltage.

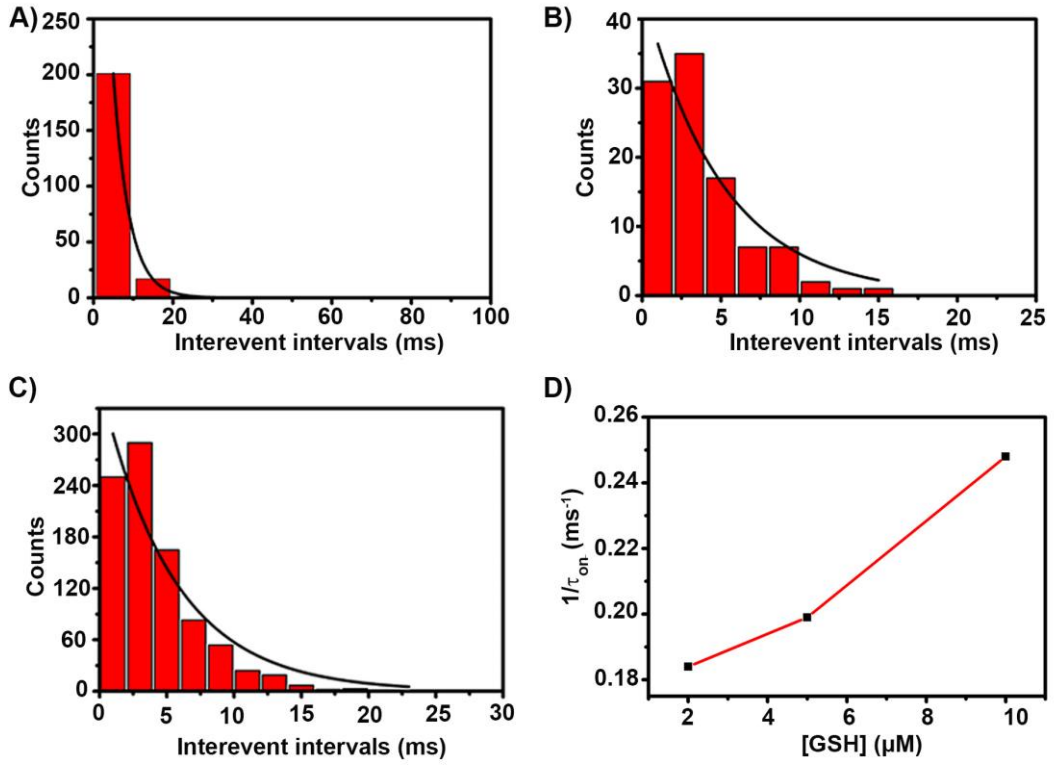

Figure S14. A), B) and C) Represented the τ_{on} of different concentrations of GSH bound within seleno-αHL nanoreactor. D) The plot of the reciprocal of τ_{on} for GSH binding events versus the GSH concentration. The mean interevent intervals time were derived from the single exponential fitting result.

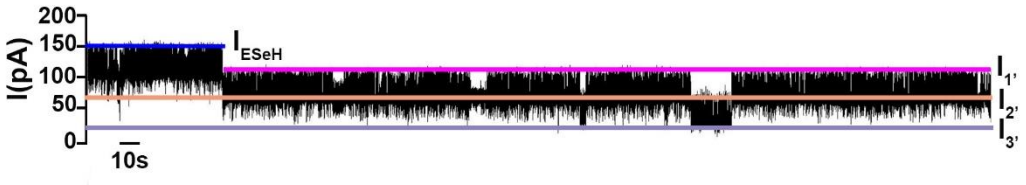

Figure S15. The single channel electric recordings based on seleno-αHL nanoreactor in the presence of GSH at a continuous applied voltage of +100 mV. The current of ESeH and different numbers of GSH reacted with ESeH, which were represented by I_{ESeH}, I_1', I_2'and I_3', respectively.

Table S3: Kinetic parameters of GSH bound with seleno-αHL based on nanopore measurements.

Number	k_{on} ($M^{-1}s^{-1}$)	k_{off} (s^{-1})	Kd (M)
1	3.833×10^{7}	8.830	2.304×10^{-7}
2	2.551×10^{7}	8.420	3.302×10^{-7}
3	2.519×10^{7}	8.550	3.390×10^{-7}